Int J Mater Form (2008) Suppl 1:499–502
DOI 10.1007/s12289-008-0150-9

Dry cutting study of an aluminium alloy (A2024-T351): a numerical and experimental approach

M. Asad, F. Girardin*, T. Mabrouki, J.-F. Rigal

LaMCoS, INSA-Lyon, CNRS UMR5259, F69621, France
**Corresponding Author: Francois.Girardin@insa-lyon.fr*

Abstract

In the present contribution, experimental and numerical methodologies concerning orthogonal cutting are proposed in order to study the dry cutting of an aeronautic aluminium alloy (A2024-T351). The global aim concerns the comprehension of physical phenomena accompanying chip formation with respect to cutting speed, such as chip segmentation and fragmentation. For experimental validation, series of tests are carried out concerning geometrical analysis of the chip; video sequences of chip formation with a high-speed camera, and high-frequency sampling measurements of the cutting force signal are realised. For the numerical approach, the material and its ductile shear failure behaviour are based on the Johnson-Cook laws. The material failure model exploited considers both damage evolution and energy coupling. Numerical results concerning cutting force and segmentation frequency are compared to experimental ones. Moreover ,an analysis of damage distributions is presented.

Keywords: Serrated chip formation, Orthogonal cutting simulation, Damage, Experimentation, A2024-T351

1 INTRODUCTION

Today, in automotive and aeronautic industries it is noted an increased request for the use of materials, which have high strength to weight ratio, for example aluminium alloys. These materials are often subjected to machining operations where the criterion of minimization of lubricant use is more and more of topicality. However, in dry (said also green) machining like the cutting of aluminium alloys, parameters of working are not yet optimised. This is mainly due to a lack of the physical phenomena comprehension accompanying the cutting operations.
In this framework, the present work point out multi-physical phenomena accompanying the cutting of the aeronautic aluminium alloy A2024-T351. The present study, deals with both a numerical approach to simulate an orthogonal cutting operation by exploiting the capabilities of ABAQUS/Explicit software and an experimental methodology for validation.

For experimental exploration, series of tests are carried out concerning geometrical analysis and measurements at high frequency sampling of cutting force signal. From the numerical point of view, a presentation of an Abaqus/Explicit methodology explains an optimised approach based on the coupling between damage and fracture energy for building an orthogonal cutting model with realistic chip formation.

2 EXPERIMENTAL APPROACH

During this work, a classical turning operation was exploited. Two working parameters were considered: the cutting speed V_c = 200-400-800 m/min and the feed rate f = 0.3-0.4-0.5 mm/rev, with a constant cutting depth a_p = 4 mm. In the following, after devices description, it is proposed to study the formation of the chip thanks to different methods: photo and video captures, and force measurements.

2.1 Experimental device

The cutting tool used is composed of an uncoated carbide insert (*CCGX 12 04 08-AL H10* fixed on tool-holder *SCLCR 2020K 12*). In order to reproduce orthogonal cutting case, the insert cutting edge is orthogonal with the feed rate and cutting speed (Kr = 90° and λ_s = 0°). Also, workpiece was prepared with concentric cylindrical grooves (figure 1).

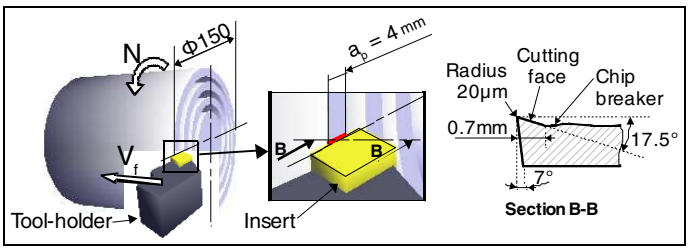

Fig. 1. Workpiece preparation

The measuring equipment is composed of a standard dynamometer (Kistler 9257B) and a high frequency data acquisition device (National Instrument NI 4472). Data treatment was developed with Matlab software. Videos were performed with a high-speed camera (MotionScope 8000 Redlake).

2.2 Analysis methodology

At first, chip morphologies were photographed using a microscope and saw-tooth shapes (segmentation) can be recognized on chips (figure 2).

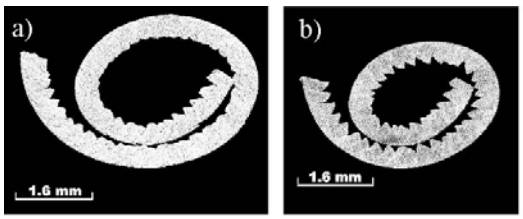

Fig. 2. Chip morphology for f=0.4 mm/rev. a) V_C=200 m/min, b) V_C = 800 m/min

Supposing incompressible material [1], segmentation and fragmentation frequencies were calculated starting from number of saw-teeth, chip thickness, chip length, feed rate and cutting speed.
Secondly, video sequences were performed. Video acquisition frequency (4 kHz) was too slow to observe chip segmentation. Nevertheless, chip fragmentation frequency can be analysed. It was determined by numbering chip fracture on the video and calculating the mean value with corresponding time. The results confirm the first evaluation from chip morphology analysis.

Finally, cutting force signal was sampled at 45 kHz. Force average value was calculated to obtain the reference level for numerical simulation comparison. The frequency spectrum was also computed. Because no correcting method was employed, such as accelerometric compensation [2] or frequency response function [3], the pass-band was limited to 1000 Hz (a third of the first dynamometer natural frequency). By investigating frequency spectrum, fragmentation frequency was localised.

2.3 Results

Table 1 gives the experimental results concerning the evolution of cutting force (Fc), fragmentation frequency and segmentation one according to cutting speed and feed rate variations.

Table 1. Experimental results

Fc(N) - Fragmentation (Hz) / *Segmentation (kHz)*			
f (mm)	Vc (m/min)		
	200	**400**	**800**
0.3	778 N	769 N	769 N
	128Hz / -	290Hz / *37.8kHz*	500Hz / *90.7kHz*
0.4	988 N	978 N	976 N
	120Hz / *10.3kHz*	351Hz / *32.4kHz*	889Hz / *64.8kHz*
0.5	1216 N	1196 N	1192 N
	256Hz / *16.2kHz*	476Hz / *22.7kHz*	1026Hz / *45.3kHz*

Those results are reference points for a numerical approach that aims at building a model which first reproduces experimental tendencies, such as chip geometry or frequencies evolution, and second, numerical values, particularly for segmentation frequency.

3 NUMERICAL APPROACH

3.1 Geometrical model and hypothesis

To improve physical comprehension, the capabilities of Abaqus/Explicit have been exploited. A 2-D orthogonal cutting model with plane strain assumption was considered. Quadrilateral continuum elements were used for a coupled temperature-displacement calculation. Interactions between contacting bodies are defined with a Coulomb's friction law [1,4]. To optimize the management of the contact between chip and cutting tool, a four-part model was developed (figure 3). Tool section shape is similar to that used in experimentation (figure 1).

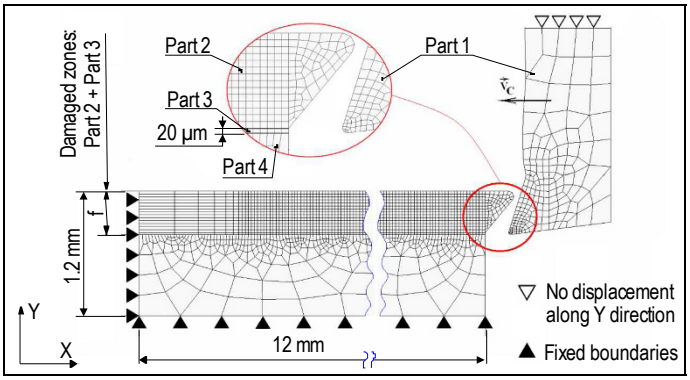

Fig. 3. Grid model and boundary conditions

3.2 Material behaviour and chip formation criterion

Johnson-Cook material model (equation (1)) is used for cutting simulation [5], and is associated with Johnson-Cook shear failure model (equation (2)) which corresponds to the damage initiation criterion.

$$\bar{\sigma} = \underbrace{\left(A + B\bar{\varepsilon}^{n}\right)}_{\substack{Elasto-plastic\\ term}} \underbrace{\left[1 + C\,ln\left(\frac{\dot{\bar{\varepsilon}}}{\dot{\bar{\varepsilon}}_0}\right)\right]}_{\substack{Viscosity\\ term}} \underbrace{\left[1 - \left(\frac{T - T_{room}}{T_{melt} - T_{room}}\right)^{m}\right]}_{\substack{Softening\\ term}} \quad (1)$$

$$\bar{\varepsilon}_{0i} = \left[D_1 + D_2 \exp\left(D_3 \frac{P}{\bar{\sigma}}\right)\right] \times \left[1 + D_4 \ln\left(\frac{\dot{\bar{\varepsilon}}}{\dot{\bar{\varepsilon}}_0}\right)\right] \left[1 + D_5\left(\frac{T - T_{room}}{T_{melt} - T_{room}}\right)\right] \quad (2)$$

where $\bar{\sigma}$ is the equivalent plastic flow stress, $\bar{\varepsilon}$ is the equivalent plastic strain, $\dot{\bar{\varepsilon}}$ is the plastic strain rate, $\dot{\bar{\varepsilon}}_0$ is the reference strain rate (1.0 s^{-1}) and $\dot{\bar{\varepsilon}}_{0i}$ is the plastic strain at damage initiation. Coefficients of laws are given table 2.

Table 2. Johnson-Cook parameter values for A2024T351 [6]

A (MPa)	B (MPa)	n	C	m
352	440	0.42	0.0083	1
D1	D2	D3	D4	D5
0.13	0.13	-1.5	0.011	0

The properties of workpiece and cutting tool are mentioned in table 3.

Table 3: Workpiece and tool physical parameters [7]

Physical parameter	Workpiece (A2024-T351)	Tool
Density, ρ *(Kg/m³)*	2700	11900
Elastic modulus, E *(GPa)*	73	534
Poisson's ratio, ν	0.33	0.22
Specific heat, C_p *(Jkg⁻¹°C⁻¹)*	$C_p = 0.557\ T + 877.6$	400
Thermal conductivity, λ *(W m⁻¹C⁻¹)*	25<T<300: $\lambda = 0.247T + 114.4$ 300<T< T_{melt} : $\lambda = -0.125T + 226.0$	50
Expansion, α_d *(µm.m⁻¹°C⁻¹)*	$\alpha_d = 8.910^{-3}T + 22.2$	×
T_{melt}, *(°C)*	520	×
T_{room}, *(°C)*	25	25

Chip formation occurs in two steps following the ductile failure phenomenon. At the beginning, the damage in element is initiated when the scalar damage parameter ω exceeds 1. This parameter is based on a cumulative law defined as:

$$\omega = \frac{\sum \Delta\bar{\varepsilon}}{\bar{\varepsilon}_{0i}} \quad (3)$$

where $\Delta\bar{\varepsilon}$ is increment of equivalent plastic strain.
In a second step, the damage evolution is specified in terms of fracture energy dissipation with a stress-displacement response thanks to Hillerborg's fracture energy proposal [8]. The fracture energy G_f used as material parameter is given by equation (4). It takes into account the characteristic length L of element to alleviate mesh dependency of the results.

$$G_f = \int_{\bar{\varepsilon}_{0i}}^{\bar{\varepsilon}_f} L\bar{\sigma}_y d\bar{\varepsilon} = \int_0^{\bar{u}_f} \bar{\sigma}_y d\bar{u} \quad (4)$$

Damage evolution law can be expressed in linear (equation (5)) or exponential form (equation (6))

$$D = \frac{L\bar{\varepsilon}}{\bar{u}_f} = \frac{\bar{u}}{\bar{u}_f} \quad (5)$$

$$D = 1 - \exp\left(-\int_0^{\bar{u}} \frac{\bar{\sigma}}{G_f} d\bar{u}\right) \quad (6)$$

where the equivalent plastic displacement at failure, $\bar{u}_f$, is computed as:

$$\bar{u}_f = \frac{2G_f}{\sigma_y} \quad (7)$$

where σ_y is the material yield stress.

4 RESULTS AND DISCUSSION

The present section deals with the mechanisms governing the chip tooth shape genesis process. The parametric studies considered are V_C = *200, 400, 800 m/min* and f = *0.4 mm/rev*. Globally experimental and numerical results such as the values of segmentation frequency and cutting force are in good comparison as shown in table 4.

Table 4. Numerical results and deviation with experiment

Vc (m/min)	200	400	800
Fc (N)	898 N – *4%*	994 N – *6%*	901 N – *8%*
Segmentation (kHz)	*Non available*	31.4 kHz – *3%*	66.3 kHz – *2%*

Figure 4 shows the distribution of damage *D* for a complete chip formation. On figure 4-c), it is remarked that this damage is localised mainly in the shearing zones and in the locations corresponding to tool/workpiece interaction. In order to bring more comprehension of chip genesis, the attention is focused on the steps characterising the formation of one chip segment.

At the beginning of chip formation, no segmentation was observed (figure 4-a)). As soon as the chip is in contact with the free surface, the segmentation phenomenon is initiated (Fig. 4-b)). This contact will increase chip curvature radius and also shear stresses in the shearing primary zone, that causes the beginning of segmentation. After a certain cutting time, the curled-up chip is subjected to high loads: those due to self-contact on chip free surface and those caused by the tool advancement. These will cause a bending state on the chip and increase locally chip damage (figure 4-d)). In comparison with video capture (figure 4-e), that may induce the chip fragmentation.

As shown by previous published papers [1], the segmentation is the result of a softening state during tool/workpiece interaction, but it can be favoured by other phenomena like pre-existing micro-cracks, machine tool vibrations or chip self-contact during its curl-up as explained previously. We can noticed that chip breaker have an important role in chip curvature, and consequently in segmentation and fragmentation.

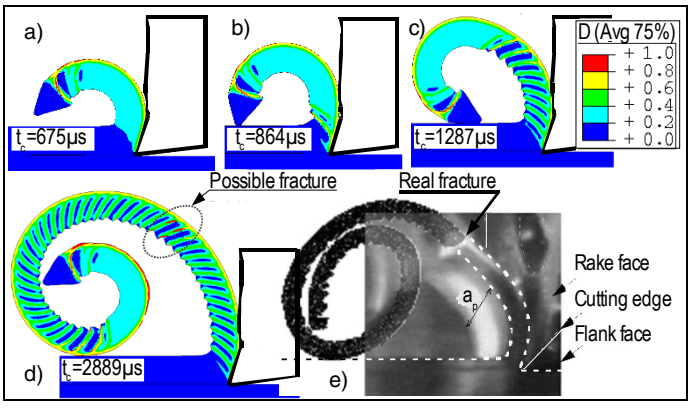

Fig. 4. Chip morphology evolution regarding to damage variable D (SDEG) and experimental comparison V_C = 200 m/min and f = 0.4 mm/rev

5 CONCLUSIONS

The global aim of this contribution concerns the comprehension physical phenomena accompanying the chip formation according to the variation of feed rate and cutting velocity for an aluminium alloy referenced as A2024-T351.

Two approaches, experimental and numerical are proposed. The experimental one focuses on physical quantity such as periodicity of chip segmentation and fragmentation. A methodology measurement of these quantities in term of frequency is proposed based on the cutting force signal analysis. From the numerical point of view, presentation of Abaqus /Explicit based methodology explains an original optimised approach for building an orthogonal cutting model with realistic chip formation. This model is based on a coupling between damage and fracture energy. The numerical results show the effect of the chip curl-up and its self contact on the initiation of segmentation. This remark was confirmed by high sampling videos.

Eventually, from a numerical point of view, the combination of the fracture energy coupling model to the Johnson-Cook law gives good results compared to the experimental ones. Values of fracture toughness Kic are often given in material databases and they can be exploited to contribute to the elaboration of a predictive cutting model.

REFERENCES

1. S. Belhadi, T. Mabrouki, J.-F. Rigal, L. Boulanouar, Experimental and numerical study of chip formation during a straight turning of hardened AISI 4340 steel. Journal of Engineering Manufacture, IMechE, PEP, London, Vol. 219, 2005, pp. 515-524
2. F. Lapujoulade, G. Coffignal, J. Pimont. Cutting forces evaluation during high speed milling, 2ème Conf. Int. IDMME'98. Compiègne – France. 27-29 May 1998.
3. L. R. Castro, P. Viéville, P. Lipinski. Correction of dynamic effects on force measurements made with piezoelectric dynamometers, International Journal of Machine Tools & Manufacture 46 (2006) 1707–1715.
4. K. Li, X.-L. Gao, J.W. Sutherland, Finite element simulation of the orthogonal metal cutting process for qualitative understanding of the effects of crater wear on the chip formation process, J. Mater. Proc. Techn. 127/3 (2002) 309–324.
5. G.R. Johnson, W.H. Cook, Fracture characteristics of three metals subjected to various strains, strain rates, temperatures and pressures, Eng. Fract. Mech. 21/1 (1985) 31–48.
6. X. Teng, T. Wierzbicki, Evaluation of six fracture models in high velocity perforation Engineering Fracture Mechanics 73 (2006) 1653–1678.
7. www.knovel.com
8. A. Hillerborg, M. Modeer, and P. E. Petersson, Analysis of Crack Formation and Crack Growth in Concrete by Means of Fracture Mechanics and Finite Elements, Cement and Concrete Research, vol. 6, pp. 773–782, 1976.